

## Special Issue

# Relationship Between Presumptive Inner Nuclear Layer Thickness and Geographic Atrophy Progression in Age-Related Macular Degeneration

Andreas Ebnetter,<sup>1,2</sup> Damian Jaggi,<sup>1</sup> Mathias Abegg,<sup>1</sup> Sebastian Wolf,<sup>1,3</sup> and Martin S. Zinkernagel<sup>1-3</sup>

<sup>1</sup>Department of Ophthalmology, Inselspital, Bern University Hospital, University of Bern, Bern, Switzerland

<sup>2</sup>Department of Clinical Research, Inselspital, Bern University Hospital, University of Bern, Bern, Switzerland

<sup>3</sup>Bern Photographic Reading Center, University of Bern, Bern, Switzerland

Correspondence: Andreas Ebnetter, Universitätsklinik für Augenheilkunde, Inselspital, CH - 3010 Bern, Switzerland; [ebnetter.andreas@gmail.com](mailto:ebnetter.andreas@gmail.com).

AE and DJ contributed equally to the work presented here and should therefore be regarded as equivalent authors.

Submitted: December 12, 2015

Accepted: April 23, 2016

Citation: Ebnetter A, Jaggi D, Abegg M, Wolf S, Zinkernagel MS. Relationship between presumptive inner nuclear layer thickness and geographic atrophy progression in age-related macular degeneration. *Invest Ophthalmol Vis Sci*. 2016;57:OCT299–OCT306. DOI:10.1167/iovs.15-18865

**PURPOSE.** To analyze inner retinal changes in patients with geographic atrophy (GA) secondary to age-related macular degeneration and identify morphological cues for progression.

**METHODS.** A total of 100 eyes with GA were assessed in this longitudinal, observational case series. Patients with GA and absent confounding pathology were compared with age-matched controls. The retinal layers on spectral-domain optical coherence tomography, acquired in tracking mode, were segmented manually on central scans through the fixation point. Zones of GA were defined based on choroidal signal enhancement from retinal pigment epithelium loss. An area of unaffected temporal retina was used for comparison. Progression of GA was quantified with fundus autofluorescence.

**RESULTS.** We analyzed 41 eyes of 41 patients (mean age  $79.2 \pm 6.7$  years). In areas of GA, the layer representing the inner nuclear layer (INL) in healthy retina was increased in thickness. Thickness of this presumptive INL was inversely correlated with best-corrected visual acuity ( $r = -0.48$ ,  $P < 0.01$ ). The presumptive INL thickness increase in atrophic areas was less marked in eyes with foveal sparing. Increased INL thickness in areas adjacent to GA was associated with a higher progression rate.

**CONCLUSIONS.** Optical coherence tomography findings demonstrate that atrophy of the retinal pigment epithelium-photoreceptor complex in GA is associated with an increase of thickness of the presumptive INL, presumably caused by remodeling of the degenerating retina. Similar alterations in the retina adjacent to areas clinically affected by GA were associated with higher atrophy progression rates.

**Keywords:** geographic atrophy, retinal segmentation, optical coherence tomography, autofluorescence, disease progression

Age-related macular degeneration (AMD), characterized by drusen and pigmentary changes, is the principal cause of irreversible vision loss in elderly in the Western world.<sup>1,2</sup> Geographic atrophy (GA) is a late-stage phenotype that results in a central scotoma of variable depth and significant visual impairment.<sup>3</sup> Macular atrophy progression is the most important determinant of visual acuity loss.<sup>4</sup> Currently, no remedy is available to slow down progression of nonexudative AMD and GA,<sup>5</sup> but such treatments may soon become available.<sup>3,6</sup> In order to maximize the cost-benefit ratio from potential treatments, it would be helpful to have parameters predicting GA progression, allowing economical allocation of medication (Zhang H, et al. *IOVS* 2015;56:ARVO E-Abstract 5149).<sup>7,8</sup>

Whereas the changes occurring in the outer retina and the retinal pigment epithelium (RPE) have been well characterized by optical coherence tomography (OCT), there is to date little information on the inner retinal layer changes in nonexudative AMD using this noninvasive imaging technology.<sup>9</sup> From histologic studies of human

donor eyes and animal models, we know that the inner layers are significantly affected by remodeling in degenerating retina, already during the early phases.<sup>10,11</sup> In absence of disease, Müller cells span almost the entire thickness of the retina, from the outer limiting to the inner limiting membrane, and have a pivotal role in retinal homeostasis.<sup>12</sup> They are among the first to respond in retinal degeneration primarily affecting the outer layers.<sup>13</sup> Due to shortcomings in resolution and reliable imaging software for automated layer delineation, it has been difficult to quantify potential changes in the inner retinal layers in the past. In recent years, however, significant improvements in retinal segmentation algorithms have been achieved, and many of the new OCT devices now have inbuilt segmentation software.<sup>14</sup> Increasing resolution and computational speed of commercially available spectral-domain (SD) devices have revolutionized the medical retina field and allow an ever more detailed longitudinal in vivo analysis of the retinal morphology in humans (Abdelfattah NS, et al. *IOVS* 2015;56:ARVO E-Abstract 892). The purpose of this study was to investigate



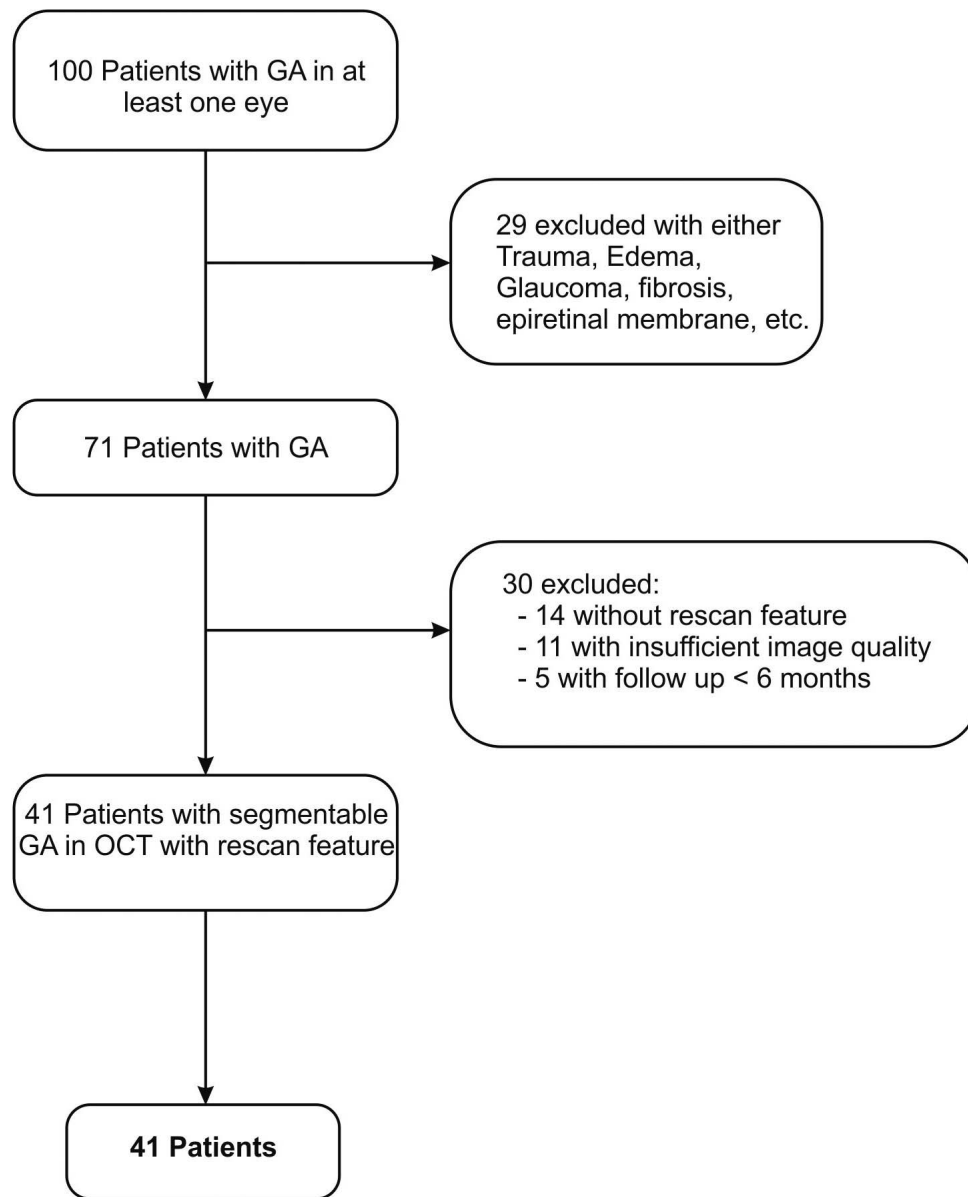


FIGURE 1. Flow diagram illustrating patient inclusion for statistical analysis.

inner retinal layer changes associated with GA, and to identify potential predictors for GA progression.

## METHODS

### Participants

This study was a retrospective, longitudinal, observational case series. Our analysis included 100 patients with GA secondary to AMD followed in the retina clinic at Bern University Hospital (Inselspital), Bern, Switzerland. The study followed the tenets of the Declaration of Helsinki, and ethics committee approval had been obtained (KEK-Nr. 370/14). The need for informed consent was waived because of the retrospective nature of the study. Study data were collected and managed using an electronic data management tool (REDCap; Vanderbilt University, Nashville, TN, USA) hosted at our institution.<sup>15</sup> The inclusion criteria were: (1) presence of GA (sharply demarcated area of RPE hypopigmentation of  $>175 \mu\text{m}$  with visible

choroidal vessels) at baseline with no evidence of choroidal neovascularization during the observational period, (2) patients aged  $\geq 50$  years, (3) follow-up of 6 months or more.<sup>16</sup> If both eyes were affected, one eye was chosen randomly by tossing a coin. Exclusion criteria (also see Fig. 1) included the evidence of retinal disease that could influence retinal layer thickness such as macular edema from diabetic retinopathy, retinal vein occlusion or other disease, pathologies of the vitreoretinal interface, hereditary retinal dystrophies, central serous chorioretinopathy, and glaucoma. Participants with foveal sparing were identified on SD-OCT.<sup>17</sup> We used 16 healthy eyes of 16 age-matched individuals as controls.

### Procedures and Imaging

All patients had undergone the following set of imaging at least twice with an OCT device (Spectralis HRA+OCT; Heidelberg Engineering, Heidelberg, Germany): combined near-infrared reflectance and SD-OCT in tracking mode; confocal scanning laser ophthalmoscopy blue light (488 nm) fundus autofluores-

cence (FAF). Furthermore, patients underwent a clinical slit-lamp examination and standardized best-corrected visual acuity (BCVA) testing. At every visit, logMAR acuity was recorded using the Early Treatment Diabetic Retinopathy Study (ETDRS) charts<sup>18</sup> and following the standard ETDRS protocol.<sup>19</sup> For SD-OCT, central scans spanning 30° of the retina involving the fixation point were performed with 28 to 36 frames averaged for each B-scan in automatic real-time (ART) mode. Additionally, standardized volume scans of the central 20° × 20° were performed consisting of 49 B-scans, with 9 to 15 frames averaged per B-scan (ART). They were used to define the anatomical center of the fovea in cases with eccentric fixation for layer thickness analysis in the central ETDRS subfield. The tracking mode allows point-to-point correlation between consecutive SD-OCT scans.

### Image Analysis

The presumptive inner nuclear layer (INL) was segmented on the central scan using commercial software (Heidelberg Eye Explorer, version 1.9.10.0). The term “presumptive” is used because architectural changes could affect segmentation. In this manuscript, the abbreviation “INL” refers to the layer on OCT segmentation that, based on the reflectance pattern, presumptively corresponds to the INL. Each central scan was corrected manually (DJ) and then validated independently by two retinal specialists (AE, MZ). In ambiguous cases, both senior investigators discussed the segmentation and reached an agreement on the final outline. The segmented images were exported (see Supplementary Methods) to ImageJ (version 1.48v) (<http://imagej.nih.gov>; provided in the public domain by the National Institutes of Health, Bethesda, MD, USA).

The borders of atrophic zones (AZ) with relevant RPE atrophy were defined based on the choroidal signal enhancement resulting from RPE loss and thinning of the outer retinal layers.<sup>17,20</sup> At the edges of GA, this signal discontinuity is generally marked and unequivocal (Fig. 2A). A temporal zone (TZ) of 1.5 mm immediately adjacent to the AZ was defined for comparison, unless this TZ was partially within 1 mm from the fixation point, in which case the starting edge of this TZ zone was defined at 1 mm from the fixation point. This was necessary to avoid flouting of data by the naturally decreased INL thickness in the fovea. If the atrophic zone was very wide, the TZ in some cases reached beyond the length of the scan image and was then less than 1.5 mm long. The average layer thicknesses (ALTs) of the INL in the AZ and the TZ were calculated by dividing the area under the curve of the INL thickness profile by the width of the respective zone. For comparison, the INL-ALTs at a comparable location were determined in an age-matched control group. To define the size of this central zone (CZ) in the controls, we calculated the average width of the AZ in the AMD-affected eyes. The central zone was centered at the fovea (Fig. 2B). In eyes with GA, we furthermore measured the ALT of the INL in the central ETDRS subfield (1 mm; red zone in Fig. 2) of the baseline scan in an analogous way to investigate associations with BCVA.

To analyze the progression of atrophy, we manually measured the GA lesion size on FAF using the region overlay tool of the Heidelberg Eye Explorer software at baseline and last follow-up. The individual yearly progression rate of the GA was calculated (see Supplementary Calculations).

### Statistical Analysis

Statistical software was used to conduct data analysis (Prism 6; GraphPad Software, Inc., La Jolla, CA, USA). Distribution of data was tested using the D’Agostino-Pearson omnibus normality test. Data of all parameters followed a Gaussian

distribution, except yearly GA progression rate. The two-sided Student’s *t*-test was used to compare means of normally distributed data. Paired analysis was done for dependent data. Linear association was quantified by calculating the Pearson correlation coefficient for normally distributed data. Otherwise, the Spearman’s rank correlation coefficient was computed. Confidence intervals were two-sided, and a *P* value of < 0.05 was considered statistically significant.

### RESULTS

We identified 100 patients with GA in at least one eye; 59 of these patients were excluded for various reasons illustrated in Figure 1. A total of 41 participants had imaging data suitable for layer segmentation and detailed analysis. The mean age ± SD of included subjects was 79.2 ± 6.7 years. Twenty patients were female, 21 male. The mean BCVA at baseline was 53.8 ± 22.9 ETDRS letters. Foveal sparing was identified in seven eyes. The mean follow-up was 36.6 ± 18.6 months. The mean size of GA at baseline and follow-up were 6.9 ± 5.5 mm<sup>2</sup> and 11.8 ± 7.0 mm<sup>2</sup>, respectively. The mean ALTs of the INL in AZ and TZ were 43.0 ± 6.6 μm and 28.6 ± 3.7 μm, respectively. The difference between ALTs was significant (*P* < 0.0001, paired *t*-test; Fig. 2A). In controls (*n* = 16), the mean age was 78.5 ± 4.2 years and the mean ALTs of the TZ- and AZ-analogue zone (CZ) were 29.0 ± 2.9 μm and 27.9 ± 3.3 μm, respectively. The difference between TZ-analogue and AZ-analogue zones was not significant in the control group (Fig. 2B). Although GA progressed over time (Fig. 3), the ALT of the INL in the AZ remained stable (43.5 ± 10.1 μm at baseline and 43.0 ± 6.4 μm at last follow-up; *P* = 0.626). When analyzing the association between INL thickness in the central ETDRS subfield and visual acuity at baseline, we detected a significant negative correlation (Pearson *r* = -0.48, *P* = 0.01, Fig. 4); increased INL thickness seemed to be linked to poor BCVA. Thirty-four eyes were included in this analysis because baseline visual acuity data was missing from seven patients. Seven eyes with foveal sparing are highlighted in Figure 4A. These eyes were excluded in a second analysis, yielding a similar outcome (Fig. 4B).

We also searched for an association between the ALT of the INL in the retina adjacent to GA (TZ) and the GA progression rate (Supplementary Figure). Figure 5 shows the positive correlation (Spearman *r* = 0.48, *P* < 0.01, *n* = 39) detected between the average INL thickness (measurements from all visits of a particular patient between baseline and last follow-up) and the yearly GA progression rate.

### DISCUSSION

The aim of this study was to investigate novel parameters from retinal layer segmentation that might predict the progression rate of GA. Previous studies have linked distinct FAF patterns,<sup>21–23</sup> drusen type (Zhang H, et al. *IOVS* 2015;56:ARVO E-Abstract 5149),<sup>24</sup> shape of the atrophic area,<sup>25</sup> specific changes of the RPE/Bruch membrane complex in SD-OCT such as outer retinal tubulations,<sup>26</sup> inner/outer segment disruption in en face imaging,<sup>27</sup> and genetic predisposition<sup>28</sup> to the progression rate of GA. The most striking finding of our analysis was marked thickening of the presumptive INL over areas of degenerated photoreceptors. Furthermore, thickening of the INL in the adjacent TZ correlated with the yearly GA progression rate. We also found a negative correlation between the presumptive INL thickness in the central ETDRS subfield and BCVA. However, this association is prone to confounding bias, since thickening of the presumptive INL is related to the presence of GA. Hence, photoreceptor loss is more likely the

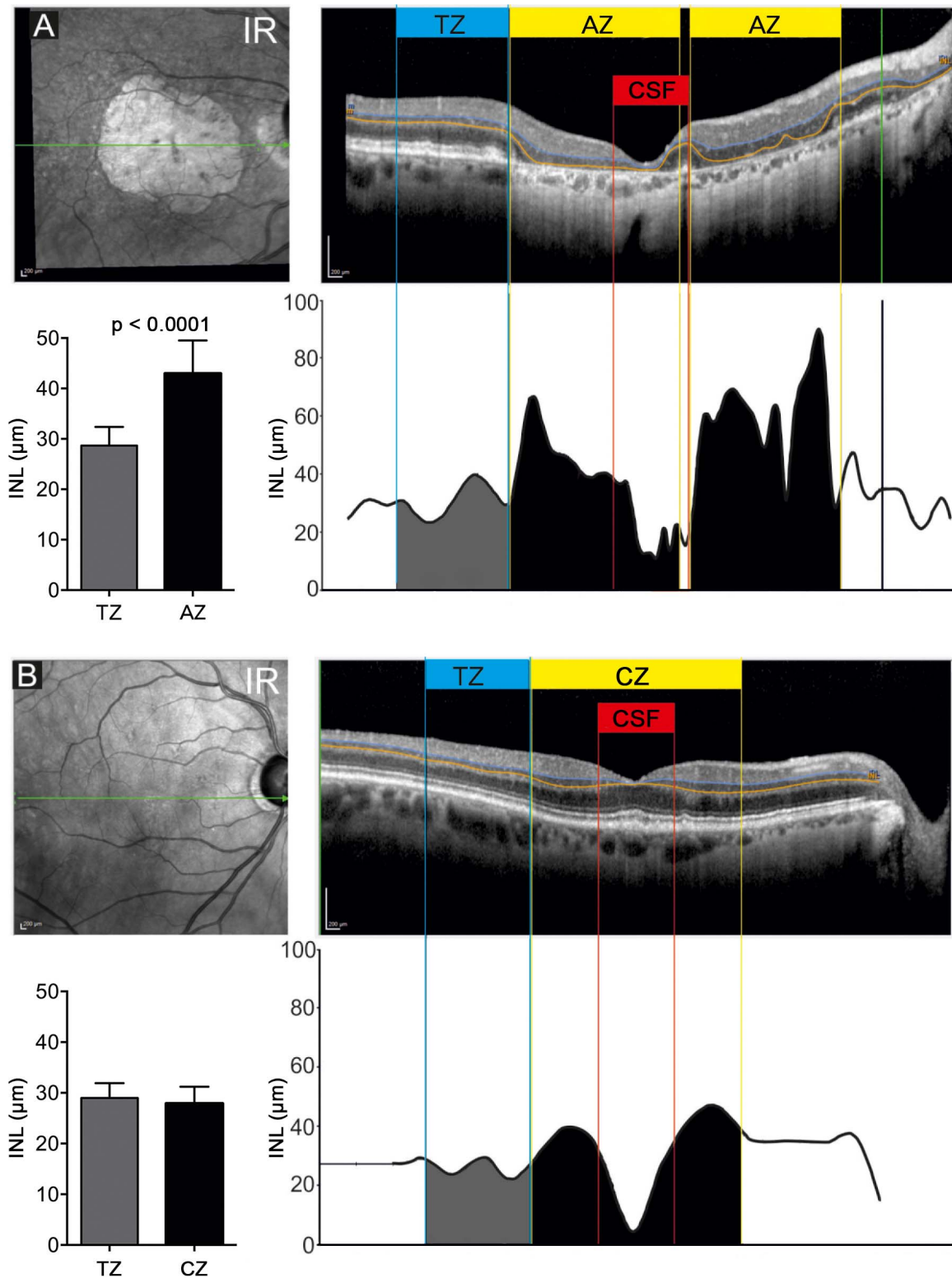


**FIGURE 2.** Illustration of segmentation protocol for quantitative analysis of the INL using SD-OCT in patients with geographic atrophy secondary to AMD and age-matched controls. (A) Near-infrared (IR) image and central SD-OCT scan of a representative patient affected by geographic atrophy with corresponding analysis of presumptive INL thickness (*bottom right*). TZ, unaffected temporal zone (width 1.5 mm); AZ, atrophic zone (GA); CSF, central ETDRS subfield. *Bottom left*: Graph showing the mean thicknesses of the INL for the AZ and the TZ. *Error bars*: standard deviation. Two-sided paired Student's *t*-test ( $n = 41$ ). (B) Scan of subject without AMD with corresponding analysis of INL thickness (*bottom right*). CZ, AZ-analogue zone. *Bottom left*: Graph showing the mean thicknesses of the INL for TZ and CZ. *Error bars*: standard deviation. Two-sided paired Student's *t*-test ( $n = 16$ ; difference not significant).

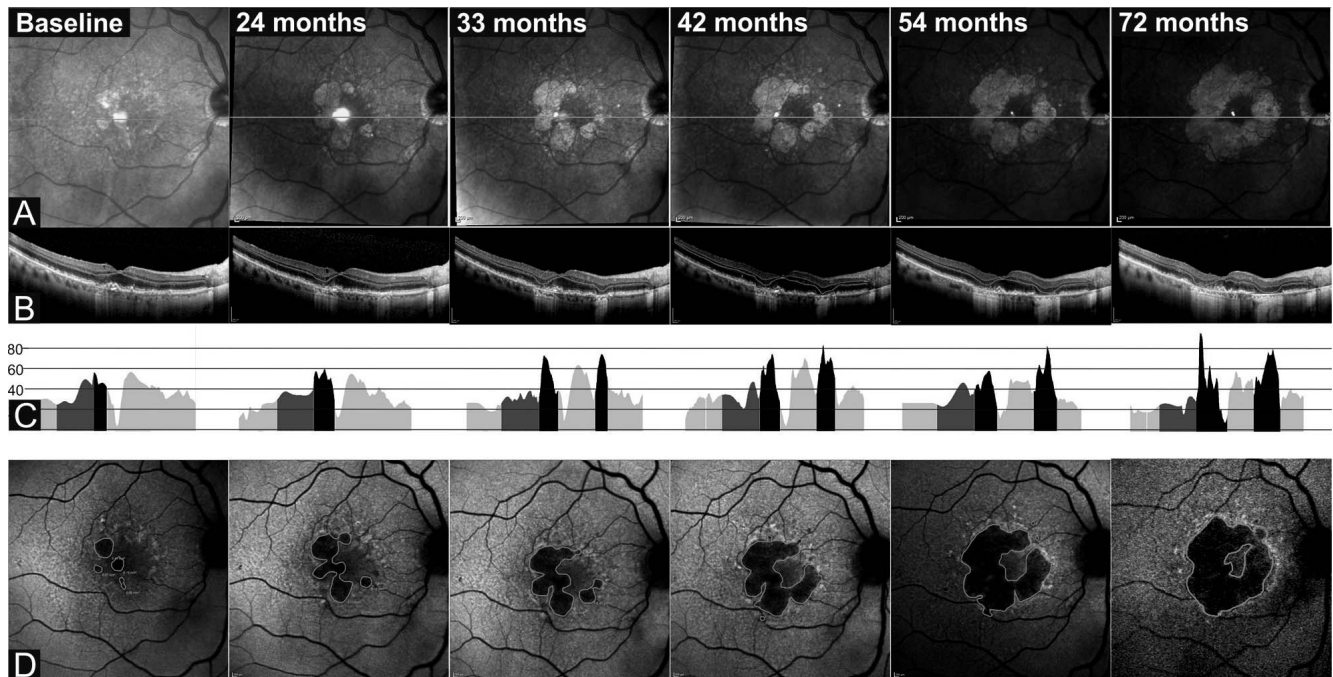


FIGURE 3. Representative images of a patient showing progression of GA with stable average thickness of the INL within the atrophic zone over 72 months. (A) Near-IR images with scan position. (B) Central SD-OCT scans with INL segmentation. (C) Corresponding INL thickness profile (atrophic zones with black shading). (D) Fundus autofluorescence images with outlined borders (green) of GA.

reason for impaired BCVA, rather than neural remodeling of the inner retinal layers.

### Remodeling of the Retina in Degeneration

Remodeling of the mammalian retina in degenerative pathology occurs in three phases and affects both the sensory (compartment limited by the basolateral tight junctions of the RPE distally and intermediate junctions formed by Müller cell apical microvilli proximally) and the neural retina (compartment between external and internal limiting membrane). While the focus of pathology during the early phases is in the sensory retina, global remodeling occurs during phase 3, significantly affecting the inner retinal layers.<sup>10</sup> Changes comprise cellular atrophy, cell death, reshaping of axonal and

dendritic trees, and transformation of glia. Gliosis is seen as either “conservative” or “proliferative reactive.” In conservative gliosis, which is supposedly neuroprotective and occurs early after insult, proliferation is absent. In the more advanced stages of degeneration with significantly impaired tissue homeostasis, Müller cells are dedifferentiated, depolarized, and proliferating.<sup>29</sup> During the remodeling process, the boundaries of the retinal compartments shift. In healthy retina the neural compartment is entirely sealed by Müller cell intermediate junctions: apical microvilli distally, foot pieces proximally, and internally by processes wrapping the blood vessels. Degeneration and disappearance of the sensory retina leads to Müller cell hypertrophy, migration, and formation of a distal fibrotic seal, which then forms the border between the retina and the equally degenerating choroid. In AMD remod-

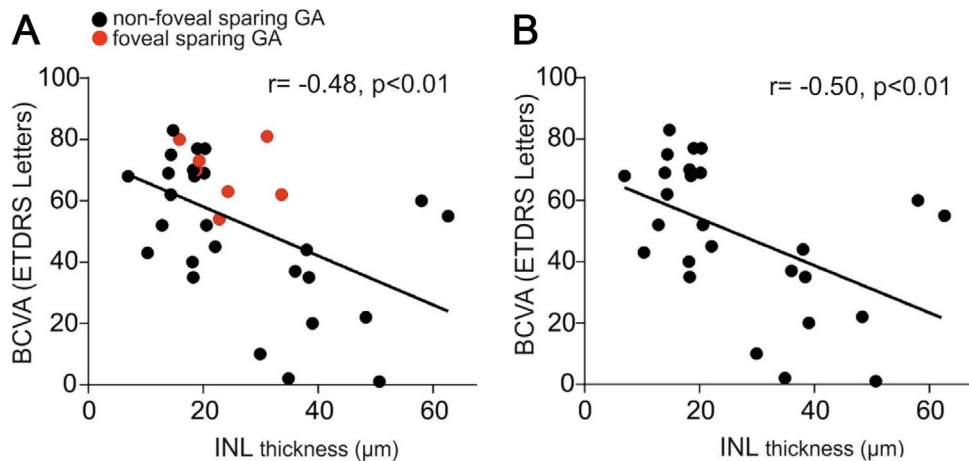


FIGURE 4. Scatterplots showing BCVA at baseline plotted against INL thickness in the central 1 mm of the central scan (corresponding to central ETDRS subfield) for individual patients. (A) All patients ( $n = 34$ ), including individuals with foveal sparing ( $n = 7$ ) marked in red (Pearson  $r = -0.48$ ;  $P < 0.01$ ). (B) Patients with foveal sparing excluded (Pearson  $r = -0.50$ ;  $P < 0.01$ ).

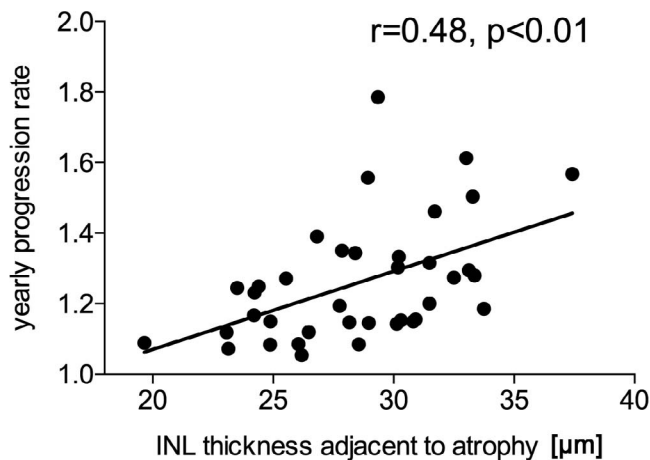


FIGURE 5. Scatterplot showing the average yearly GA progression rate plotted against the average INL thickness (mean of all measurements between baseline and last follow-up from a particular patient) of the temporal 1.5 mm zone immediately adjacent to the atrophic zone ( $n = 39$ , Spearman  $r = 0.48$ ;  $P < 0.01$ ).

eling, Müller cells increasingly express intermediate filaments like vimentin and glial fibrillary acidic protein.<sup>30</sup> Extracellular matrix changes characterized by depositions of proteoglycans and altered composition have previously been reported to be associated with the pathogenesis of AMD.<sup>31</sup> Migration of RPE into the retina also occurs in advanced pathology. Such profound modification of the retinal architecture might alter the signaling properties of the retina in OCT, which is based on reflective index changes in the tissue. Therefore, it seems prudent to use the adjective “presumptive” when referring to the INL in severely degenerated retina. The crude layer thickness measurement by OCT currently does not allow drawing conclusions on the exact composition and cellular content of tissue, nor function or biochemical changes at the cellular level. Nevertheless, the observed thickening of the presumptive INL in areas of GA is most likely closely related to tissue remodeling and can be used as a surrogate marker for functional loss of the fovea.

### Spreading Patterns and Role of Adjacent INL

From histological assessment of human eyes with GA, we know that in AMD photoreceptor loss precedes degeneration and atrophy of the RPE<sup>32</sup> and rods are affected earlier than cones.<sup>33,34</sup> Retina adjacent to areas of GA histologically shows different levels of subclinical damage. Different transition patterns exist both clinically<sup>35,36</sup> and histologically<sup>37</sup> at the edges of GA. While in the abrupt pattern—present in a minority of eyes—both photoreceptor segments are simultaneously affected, most eyes display a more gradual transition characterized by outer segment loss but variably preserved inner segments. In these eyes, the zone with histological abnormalities extends as far as approximately 1500 μm distally.<sup>37</sup> The role of the surrounding retinal tissue in predicting GA progression has been investigated by several groups.<sup>35,38,39</sup> Geographic atrophy generally spreads in a centrifugal pattern. Growth characteristics of GA can be predicted by specific FAF patterns, which have previously been described.<sup>21,23,40,41</sup> Functional methods have also been shown to be useful in predicting GA progression.<sup>42-44</sup> However, focal differences exist sometimes in a single eye, which suggests a substantial influence of local factors.<sup>45</sup> In the subgroup of patients with foveal sparing, GA spread is significantly greater in the centrifugal than the centripetal

direction.<sup>46</sup> In these individuals, the fovea is affected by atrophy only late in the course of the disease, which results in relatively well-preserved central vision despite gradually enlarging paracentral visual field defects. In the current series, we found an association between INL thickness in the retina adjacent to GA and progression. This suggests that inner retina homeostasis disturbance and remodeling occur before GA becomes clinically evident. Meticulous assessment of these adjacent areas might produce meaningful clues to predict general and local atrophy progression.

### Study Limitations

Limitations of this study include the small sample size and the retrospective design, which allows detection of associations only. However, the acquisition of the data and imaging was done in a very standardized fashion with a single specific SD-OCT device. Secondly, the central OCT scans always included the fixation point of the individual, which in GA affecting the fovea is often located eccentrically, and not coinciding with the anatomical foveola. Therefore, the variability of layer thicknesses is arguably increased. The definition of GA in this manuscript was based on choroidal hypertransmission in OCT, which may have led to the inclusion of cases with RPE depigmentation only, rather than real GA with RPE atrophy. More sophisticated, possibly more accurate definitions exist.<sup>8</sup> Finally, the TZ used as internal control could have been already subclinically altered, since it corresponds to about the area of retina adjacent to GA in which histological evidence of early degeneration can be found.<sup>37</sup> However, the INL thickness in this zone (TZ) was similar to age-matched controls.

In conclusion, in this retrospective case series, we found that increased thickness of the presumptive INL within areas of GA was associated with poor visual acuity. However, confounding may well be present since the INL thickness changes are associated with photoreceptor degeneration. Increased INL thickness in the retina immediately adjacent to the edges of GA was associated with a higher progression rate of GA. Information on expected atrophy progression might be helpful in allocating future treatments for nonexudative AMD to suitable patients, and reduce costs for health care systems as well as treatment burden for patients (Abdelfattah NS, et al. *IOVS* 2015;56:ARVO E-Abstract 892). However, prospective studies would be needed to corroborate our findings.

### Acknowledgments

Supported by the Swiss National Science Foundation (MSZ; grant 320030\_156019) and by Foundation OPOS, Stiftung zugunsten von Wahrnehmungsbehinderten, St. Gallen, Switzerland (AE, MSZ).

Disclosure: **A. Ebnetter**, Allergan (C, R), Bayer (R), Novartis (R); **D. Jaggi**, None; **M. Abegg**, None; **S. Wolf**, Allergan (F, C), Bayer (F, C), Heidelberg Engineering (F, C), Novartis (F, C), Roche (F, C), Optos (F, C), Zeiss (F, C), Euretina (S); **M.S. Zinkernagel**, Bayer (F, C), Heidelberg Engineering (F), Novartis (C, D)

### References

1. Friedman DS, O'Colmain BJ, Munoz B, et al. Prevalence of age-related macular degeneration in the United States. *Arch Ophthalmol*. 2004;122:564-572.
2. Wong WL, Su X, Li X, et al. Global prevalence of age-related macular degeneration and disease burden projection for 2020 and 2040: a systematic review and meta-analysis. *Lancet Glob Health*. 2014;2:e106-e116.
3. Holz FG, Strauss EC, Schmitz-Valckenberg S, van Lookeren Campagne M. Geographic atrophy: clinical features and

- potential therapeutic approaches. *Ophthalmology*. 2014;121:1079-1091.
4. Sunness JS, Gonzalez-Baron J, Applegate CA, et al. Enlargement of atrophy and visual acuity loss in the geographic atrophy form of age-related macular degeneration. *Ophthalmology*. 1999;106:1768-1779.
  5. Jaffe GJ, Schmitz-Valckenberg S, Boyer D, et al. Randomized trial to evaluate tansporine in geographic atrophy secondary to age-related macular degeneration: the GATE Study. *Am J Ophthalmol*. 2015;160:1226-1234.
  6. Meleth AD, Wong WT, Chew EY. Treatment for atrophic macular degeneration. *Curr Opin Ophthalmol*. 2011;22:190-193.
  7. Ho AC, Busbee BG, Regillo CD, et al. Twenty-four-month efficacy and safety of 0.5 mg or 2.0 mg ranibizumab in patients with subfoveal neovascular age-related macular degeneration. *Ophthalmology*. 2014;121:2181-2192.
  8. Wykoff CC, Croft DE, Brown DM, et al. Prospective trial of treat-and-extend versus monthly dosing for neovascular age-related macular degeneration: TREX-AMD 1-year results. *Ophthalmology*. 2015;122:2514-2522.
  9. Abdelfattah NS, Sadda S. Dry AMD progression in wet AMD: what we know and don't know about geographic atrophy. Available at: <http://www.retina-specialist.com/article/dry-amd-progression-in-wet-amd>. Accessed February 15, 2016.
  10. Marc RE, Jones BW, Watt CB, Strettoi E. Neural remodeling in retinal degeneration. *Prog Retin Eye Res*. 2003;22:607-655.
  11. Marc RE, Jones BW, Watt CB, Vazquez-Chona F, Vaughan DK, Organisciak DT. Extreme retinal remodeling triggered by light damage: implications for age related macular degeneration. *Mol Vis*. 2008;14:782-806.
  12. Bringmann A, Pannicke T, Grosche J, et al. Müller cells in the healthy and diseased retina. *Prog Retin Eye Res*. 2006;25:397-424.
  13. Jones BW, Pfeiffer RL, Ferrell WD, Watt CB, Marmor M, Marc RE. Retinal remodeling in human retinitis pigmentosa. *Exp Eye Res*. In press.
  14. Waldstein SM, Gerendas BS, Montuoro A, Simader C, Schmidt-Erfurth U. Quantitative comparison of macular segmentation performance using identical retinal regions across multiple spectral-domain optical coherence tomography instruments. *Br J Ophthalmol*. 2015;99:794-800.
  15. Harris PA, Taylor R, Thielke R, Payne J, Gonzalez N, Conde JG. Research electronic data capture (REDCap)—a metadata-driven methodology and workflow process for providing translational research informatics support. *J Biomed Inform*. 2009;42:377-381.
  16. Yehoshua Z, Rosenfeld PJ, Gregori G, et al. Progression of geographic atrophy in age-related macular degeneration imaged with spectral domain optical coherence tomography. *Ophthalmology*. 2011;118:679-686.
  17. Sayegh RG, Simader C, Scheschy U, et al. A systematic comparison of spectral-domain optical coherence tomography and fundus autofluorescence in patients with geographic atrophy. *Ophthalmology*. 2011;118:1844-1851.
  18. Ferris FL III, Kassoff A, Bresnick GH, Bailey I. New visual acuity charts for clinical research. *Am J Ophthalmol*. 1982;94:91-96.
  19. Early Treatment Diabetic Retinopathy Study Research Group. Photocoagulation for diabetic macular edema. Early Treatment Diabetic Retinopathy Study report number 1. *Arch Ophthalmol*. 1985;103:1796-1806.
  20. Schmitz-Valckenberg S, Fleckenstein M, Gobel AP, Hohman TC, Holz FG. Optical coherence tomography and autofluorescence findings in areas with geographic atrophy due to age-related macular degeneration. *Invest Ophthalmol Vis Sci*. 2011;52:1-6.
  21. Biarnes M, Arias L, Alonso J, et al. Increased fundus autofluorescence and progression of geographic atrophy secondary to age-related macular degeneration: The GAIN Study. *Am J Ophthalmol*. 2015;160:345-353.e5.
  22. Holz FG, Bindewald-Wittich A, Fleckenstein M, et al. Progression of geographic atrophy and impact of fundus autofluorescence patterns in age-related macular degeneration. *Am J Ophthalmol*. 2007;143:463-472.
  23. Jeong YJ, Hong IH, Chung JK, Kim KL, Park SP. Predictors for the progression of geographic atrophy in patients with age-related macular degeneration: fundus autofluorescence study with modified fundus camera. *Eye (Lond)*. 2014;28:209-218.
  24. Nittala MG, Ruiz-Garcia H, Sadda SR. Accuracy and reproducibility of automated drusen segmentation in eyes with non-neovascular age-related macular degeneration. *Invest Ophthalmol Vis Sci*. 2012;53:8319-8324.
  25. Domalpally A, Danis RP, White J, et al. Circularity index as a risk factor for progression of geographic atrophy. *Ophthalmology*. 2013;120:2666-2671.
  26. Moussa K, Lee JY, Stinnett SS, Jaffe GJ. Spectral domain optical coherence tomography-determined morphologic predictors of age-related macular degeneration-associated geographic atrophy progression. *Retina*. 2013;33:1590-1599.
  27. Nunes RP, Gregori G, Yehoshua Z, et al. Predicting the progression of geographic atrophy in age-related macular degeneration with SD-OCT en face imaging of the outer retina. *Ophthalmic Surg Lasers Imaging Retina*. 2013;44:344-359.
  28. Grassmann F, Fleckenstein M, Chew EY, et al. Clinical and genetic factors associated with progression of geographic atrophy lesions in age-related macular degeneration. *PLoS One*. 2015;10:e0126636.
  29. Bringmann A, Francke M, Pannicke T, et al. Role of glial K(+) channels in ontogeny and gliosis: a hypothesis based upon studies on Müller cells. *Glia*. 2000;29:35-44.
  30. Wu KH, Madigan MC, Billson FA, Penfold PL. Differential expression of GFAP in early v late AMD: a quantitative analysis. *Br J Ophthalmol*. 2003;87:1159-1166.
  31. Nita M, Strzalka-Mrozik B, Grzybowski A, Mazurek U, Romaniuk W. Age-related macular degeneration and changes in the extracellular matrix. *Med Sci Monit*. 2014;20:1003-1016.
  32. Sarks JP, Sarks SH, Killingsworth MC. Evolution of geographic atrophy of the retinal pigment epithelium. *Eye (Lond)*. 1988;2:552-577.
  33. Jackson GR, Owsley C, Curcio CA. Photoreceptor degeneration and dysfunction in aging and age-related maculopathy. *Ageing Res Rev*. 2002;1:381-396.
  34. Owsley C, McGwin G Jr, Jackson GR, Kallies K, Clark M. Cone- and rod-mediated dark adaptation impairment in age-related maculopathy. *Ophthalmology*. 2007;114:1728-1735.
  35. Bearely S, Chau FY, Koreishi A, Stinnett SS, Izatt JA, Toth CA. Spectral domain optical coherence tomography imaging of geographic atrophy margins. *Ophthalmology*. 2009;116:1762-1769.
  36. Wolf-Schnurrbusch UE, Enzmann V, Brinkmann CK, Wolf S. Morphologic changes in patients with geographic atrophy assessed with a novel spectral OCTSLO combination. *Invest Ophthalmol Vis Sci*. 2008;49:3095-3099.
  37. Bird AC, Phillips RL, Hageman GS. Geographic atrophy: a histopathological assessment. *JAMA Ophthalmol*. 2014;132:338-345.
  38. Fleckenstein M, Charbel Issa P, Helb HM, et al. High-resolution spectral domain-OCT imaging in geographic atrophy associated with age-related macular degeneration. *Invest Ophthalmol Vis Sci*. 2008;49:4137-4144.
  39. Fleckenstein M, Schmitz-Valckenberg S, Martens C, et al. Fundus autofluorescence and spectral-domain optical coherence tomography characteristics in a rapidly progressing form

- of geographic atrophy. *Invest Ophthalmol Vis Sci.* 2011;52:3761-3766.
40. Schmitz-Valckenberg S, Bindewald-Wittich A, Dolar-Szczasny J, et al. Correlation between the area of increased autofluorescence surrounding geographic atrophy and disease progression in patients with AMD. *Invest Ophthalmol Vis Sci.* 2006;47:2648-2654.
  41. Schmitz-Valckenberg S, Fleckenstein M, Scholl HP, Holz FG. Fundus autofluorescence and progression of age-related macular degeneration. *Surv Ophthalmol.* 2009;54:96-117.
  42. Luu CD, Dimitrov PN, Robman L, et al. Role of flicker perimetry in predicting onset of late-stage age-related macular degeneration. *Arch Ophthalmol.* 2012;130:690-699.
  43. Midena E, Vujosevic S, Convento E, Manfre A, Cavarzeran E, Pilotto E. Microperimetry and fundus autofluorescence in patients with early age-related macular degeneration. *Br J Ophthalmol.* 2007;91:1499-1503.
  44. Phipps JA, Dang TM, Vingrys AJ, Guymer RH. Flicker perimetry losses in age-related macular degeneration. *Invest Ophthalmol Vis Sci.* 2004;45:3355-3360.
  45. Fleckenstein M, Schmitz-Valckenberg S, Adrion C, et al. Tracking progression with spectral-domain optical coherence tomography in geographic atrophy caused by age-related macular degeneration. *Invest Ophthalmol Vis Sci.* 2010;51:3846-3852.
  46. Lindner M, Boker A, Mauschwitz MM, et al. Directional kinetics of geographic atrophy progression in age-related macular degeneration with foveal sparing. *Ophthalmology.* 2015;122:1356-1365.